



HAL
open science

Innovative sodium fast reactors control rod designs

H. Guo, L. Buiron

► **To cite this version:**

H. Guo, L. Buiron. Innovative sodium fast reactors control rod designs. 4th GIF Symposium - The Generation IV International Forum, Oct 2018, Paris, France. cea-02338548

HAL Id: cea-02338548

<https://cea.hal.science/cea-02338548>

Submitted on 24 Feb 2020

HAL is a multi-disciplinary open access archive for the deposit and dissemination of scientific research documents, whether they are published or not. The documents may come from teaching and research institutions in France or abroad, or from public or private research centers.

L'archive ouverte pluridisciplinaire **HAL**, est destinée au dépôt et à la diffusion de documents scientifiques de niveau recherche, publiés ou non, émanant des établissements d'enseignement et de recherche français ou étrangers, des laboratoires publics ou privés.

INNOVATIVE SODIUM FAST REACTORS CONTROL ROD DESIGNS

Hui Guo⁽¹⁾, Laurent Buiron⁽²⁾

(1) Hui Guo - CEA, DEN, Cadarache, DER, SPRC, F-13-108 Saint-Paul-Lez-Durance, France
Tel: +33(0)04-42-25-42-28, Email: hui.guo@cea.fr

(2) Laurent Buiron - CEA, DEN, Cadarache, DER, SPRC, F-13-108 Saint-Paul-Lez-Durance, France
Tel: +33(0)04-42-25-21-66, Email: laurent.buiron@cea.fr

I. INTRODUCTION

To guide the next generation fast reactor design, GIF defined global objectives in terms of safety improvement, sustainability, economy, non-proliferation and physical-protection [1]. Sodium Fast Reactor (SFR) is studied as potential industrial G-IV reactors in France. Many efforts in CEA have been made to achieve these challenging technological criteria [2]–[5].

Next generation self-breeder sodium fast reactors exhibit relatively low reactivity swing compared to past concepts, with the consequence that the core control rods have to be adapted to fulfil both reactivity control requirements, power map distribution and safety requirements[5]–[8]. The optimal design of such control systems is a complex and challenging task, as it involves a large set of target criteria and constraints to be simultaneously met, including boron depletion with irradiation, power peak localization and maximum linear heat rate estimation, core shutdown margin, etc.

The most widely employed technique to control the core's reactivity in fast reactors is by inserting or removing absorber materials[9]. Boron, present in the form of boron carbide, B₄C, is the most generally used absorber in SFR because its relatively high neutron absorption cross-sections. The ceramic B₄C is available with relative low price with comparative ease of fabrication. Its simple reaction chain also raises the degradation of its reactivity worth especially for B₄C with low ¹⁰B enrichment.

Currently, the absorber materials are enclosed in absorber pins and then packaged in

movable cluster in controls rods sub-assembly. Although many improvements are achieved for design of control rods with B₄C as absorber, its residence is still limited by effects of irradiation on B₄C: helium generation, decrease of thermal conductivity and pellet swelling. The burn-up of ¹⁰B at 210×10²⁰ at./cm³ generate 777 cm³ of helium at standard pressure and hence its loading on the control clad would be important if the closed pin design is used. This could be solved by providing sufficient plenum volume or by using venting pin design. The venting pin design increases the thermal transfer but at same time diffusion of carbon to the steel structure i.e. pin clad. The melting temperature is higher than 2350 °C but its chemical reaction with steel starts from 1000 °C and becomes not acceptable beyond 1200 °C[10]. The thermal conductivity decreases with increase of temperature (after a pic at about 100 °C), ¹⁰B enrichment and also the depth of irradiation. Under the irradiation, the thermal conductivity decreases and hence the thermal conductivity which will reduce its margin to melting temperature[11]. The irradiation also raises swelling of ceramic pellet which will finally trigger the Absorber-Clad Contact (ACC) which is the principal effect limit the residence time of control rods in the core. In order to retard the swelling, the pellet with B₄C is enwrapped in steel shroud. And hence the maximal burn-up of ¹⁰B is increased from 150×10²⁰ at./cm³ (without shroud) to 210×10²⁰ at./cm³ according to experiences from PHENIX and SUPER-PHENIX reactors.

After a preliminary study, there are several innovative designs directions to improve performance of control rods such as optimized

pins size, alternative absorber materials, and application of moderators. These designs possess potentials to improve its neutronic characteristics safety margin, economical performance while its complete analysis requires notably more accurate calculation of efficiency and evolution of isotopes' concentrations under irradiation. At same time, a determinist transport code called APOLLO3 is under development at CEA and it will replace ERANOS code[12] for fast reactors analysis. Unstructured adaptive mesh SN solvers (MINARET)[13], as well as 2D and 3D Method of Characteristic's (MOC) are already implemented in APOLLO3[14]. An important effort is invested to develop and validate schemes in APOLLO3. This recent neutronic transport code improves the simulation of control rods sub-assemblies in G-IV fast reactors and also for some challengeable design works.

II. INNOVATIVE DESIGN DIRECTIONS

According to previous study based on typical GIV-SFR, the margin to melting would limit largely the residence time of current control rods designs if high ^{10}B enrichment B_4C is used[15]. Hence, smaller pin size control rods are proposed to increase the margin to melting after irradiation by means of liner heat rating reduction. However, these works are based on ERANOS codes and more detailed and accurate study is needed.

Different designs of control rods with B_4C are investigated under irradiation of typical G-IV SFR spectrum with Monte-Carlo (MC) TRIPOLI-4 code[16]. Fig 1 shows their distribution of ^{10}B absorption reaction rate and Form Factor (FF) is the ratio between maximal absorption rate and average absorption rate. Fig 1.a is the current control rods design where the reaction rate decreases largely from the absorber in the outer region to the inner region. Fig 1.b and Fig 1.c keep the same absorber volume as Fig 1.a but increase the number of pins. As show from Fig 1.a to Fig 1.c, the gradient of absorption becomes more important with decrease of pins' radius that may induce depletion pic in certain

region and hence decrease its safety margin or limit its residence time.

As the absorption ability of these materials decreases with neutron energy, utilization of moderator seems to be a good option to increase their reactivity worth or optimize reaction distribution. Several moderator materials are considered in this works. ZrH_2 is a good moderator because it contains two light hydrogen nuclei. Nevertheless, the dissociation temperature of ZrH_2 is very close the operation temperature of core[17]. In the future, the suitable stoichiometry of hydrogen should be considered and other hydrides with higher desorption temperature may be also studied. The reason to give the preference to oxide, such as BeO and MgO , is their high fusion temperature.

Small pin designs also offer the flexibility to introduce moderator. As shown the white regions in Fig 1.d-f, certain B_4C pins in Fig 1.c are replaced by pins with moderator material. With less investment of absorber material, the use of moderator increases slightly the reactivity worth of control rods with higher average absorption rate. Furthermore, absorption distribution of ^{10}B become more homogenize with use of moderator. However, evaluation of these designs in the core is required.

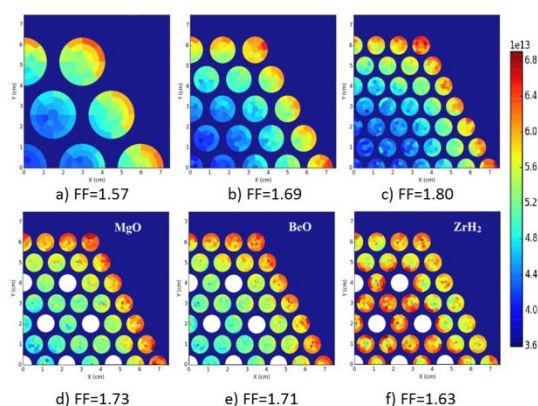


Fig 1. ^{10}B Absorption Reaction Rate Distribution

One main function of control rods is to compensate reactivity loss during operating cycle. This requires important reactivity worth of control rods with only a small part inserted which limits the selection of absorber materials. G-IV industrial size SFR designs leads to reduce

the reactivity loss to minimize inadvertent Control Rod Withdrawal (CRW) effects. At same time, this improvement enables the use of some other absorbers with less absorption ability but with advantage in other aspects. Hafnium, Gadolinium, Europium absorb neutron by (n, γ) reaction that generates less heat by comparing with B_4C and without any gas release. Furthermore, some materials such as metallic Hf and HfB₂ have better heat transfer ability and hence lower temperature in the centre of absorber[18]. These properties give the intuitive safety characteristics to control rods. In addition, their long depletion reaction chains would reduce its disappearance kinetic and hence increase their residence time. In this work, we validate their neutronic simulation method firstly and then investigate their candidate forms: Gd₂O₃, Eu₂O₃, Dy₂TiO₅, Hf, HfH_{1.62} and HfB₂.

III. METHODOLOGY

Accurate and high performance neutronic simulation is the key for the evaluation of these innovative designs of reactivity control system. The complex geometries of control rods should be treated in details because control rods is the most sub-critical structures in the core and hence with important flux gradient. The complex chains for different isotope should also be considered for their depletion calculation. After careful weighting of advantages and disadvantages of different tools, APOLLO3 is chosen for the neutronic simulation of these reactivity control systems design works.

The calculation scheme in this deterministic code includes two steps from lattice calculation to core calculation. The MOC based lattice calculation is able to simulate complex geometries wit exact description thereby compute self-shielding effects in this step. The tabulated cross-section scheme improves significantly the accuracy of depletion calculation because it's able to transfer the variation on self-shielding from lattice step to core step, which is important for the absorber materials. Different from homogenous description of all structures in traditional

deterministic codes, a heterogeneous description of control rods is proposed because MINARET is able to treat unstructured geometry. Such heterogeneous description improves further the accuracy but it needs more calculation time. Our development and validation works prove APOLLO3 has high level confidence to be used for innovative control rod designs[19].

By comparing with EFR and SUPER-PHENIX core types, SFR-V2B (3600 MWth) was the result of optimization process especially toward reduced reactivity loss and sodium void effect. This concept is based on a bundle of tightly packed and large-diameter fuel pins designed to increase the fuel fraction in the core while reducing the sodium fraction[5], [20]. A reduction in the core volume power density was found to be the best solution for meeting the requested design parameters that imply a reduction of the sodium volume fraction together with an increase of the fuel volume fraction. SFR-V2B is a representative GIV SFR core and hence is chosen in this works. As shown in Fig 2, SFR-V2B has 267 inner core S/A and 186 outer core S/A. After one cycle irradiation, 410 EFPD, about 1/5th fuel are recycled. The reactivity loss of SFR-V2B is about 450 pcm per equilibrium cycle.

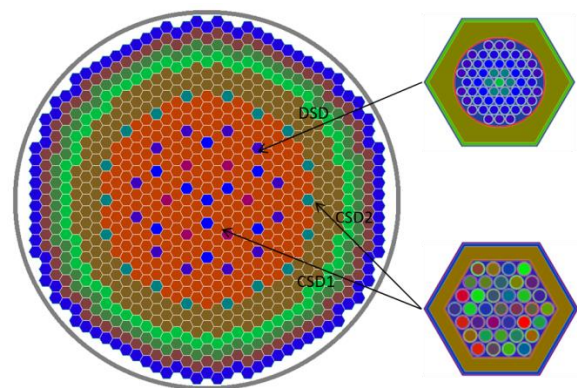


Fig 2. Layout of SFR-V2B core and its original control rods designs

SFR-V2B has two independent control rods systems. The first system is designed for the operation of reactor (power management, burn-up compensation...) and also for shutdowns needs. This system is named CSD (Control Shutdown System) in SFR-V2B projects. This system include 24 control rods sub-assemblies:

the first part CSD1 has 6 sub-assemblies which locate in the inner core and the second part CSD2 has 18 sub-assemblies that locate in the interface between inner and outer core. The second system is dedicated to the emergency shutdown. This system is named DSD (Diverse Shutdown System) which include 12 sub-assemblies. CSD and DSD are redundant, independent, and diverse in order to ensure a safe shutdown of a reactor at any time needed.

At Beginning of Equilibrium Cycle (BOEC), the core is set at critical state where CSD1 and DSD are kept at the top of fissile zone while CSD2 inserted about 25 cm into fissile zone. After one cycle irradiation, CSD is also completely withdrawn to compensate core's reactivity loss. The reactivity worth of CSD2 critical insertion is hence its ability to compensate reactivity loss. The reactivity worth of all control rods insertion at bottom of fissile zone is used to bring core from full power state to isothermal shutdown that includes: Doppler Effect (~ 1000 pcm); management of fuel handling errors (~ 2000 pcm); reactivity loss (~ 450 pcm); integration of uncertainty level (~ 750 pcm). That means the anti-reactivity of all control rods insertion should be higher than 4200 pcm. The original designs of CSD and DSD S/A are also shown in Fig 2. CSD was based B_4C and DSD use 90 % ^{10}B enrichment B_4C . The geometries for sub-assembly calculation of SFR-V2B using APOLLO3 are shown in Fig 3. The sub-assembly is normalized 50 W/g(HN) in fuel region with total irradiation time 3000 EFPD.

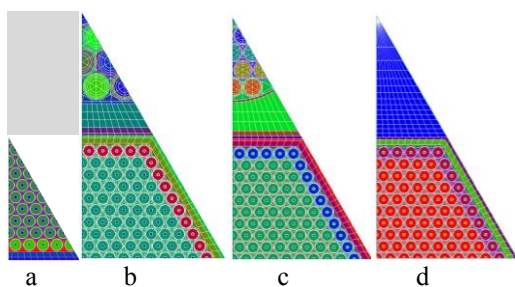


Fig 3. Geometries for SFR-V2B sub-assembly calculation a) 1/12th of Fuel sub-assembly. b) 1/12th CSD-Fuel cluster. c) 1/12th DSD-Fuel cluster. d) 1/12th Reflector-Fuel cluster.

In the core level calculation, two methods indicated previously, i.e. CR-HOMO and CR-

HETE, are compared. These control rods are used for 5 cycles with total irradiation time 2050 EFPD. The efficiency in Table 1 is the reactivity worth of 25 cm insertion of CSD2 at BOEC. In this work, the Beginning of Life (BOL) for these control rods is 0 EFPD where all rods use new materials and the End of Life (EOL) is 2050 EFPD.

As shown in Table 1, for both original designs with natural B_4C and materials with absorption resonance and moderators, CR-HOMO scheme shows high coherence with CR-HETE scheme not only on the efficacy but also on its variation. Note that CR-HETE requires 6 times computation time as CR-HOMO. In following works, CR-HOMO is used and in the future the ideal candidate designs will be recomputed with CR-HETE scheme.

Table 1. Benchmark between CR-HETE and CR-HOMO

EFPD	Natural B_4C		$HfH_{1.62}$	
	HOMO	HETE	HOMO	HETE
0	509	510	672	665
410	491	493	659	652
820	483	484	659	651
1230	463	464	651	643
1640	445	447	646	647
2050	430	432	642	636

IV. RESULTS AND DISCUSSIONS

IV.A. Different ^{10}B enrichment

In this section, the absorber in Fig 3.b is replaced by different enrichment ^{10}B to compute their effective microscopic cross-section using APOLLO3-TDT solver.

Fig 4 shows the variation of one-group effective microscopic absorption cross-section of ^{10}B with concentration. The microscopic cross-section decreases with increase of ^{10}B concentration because of the increase of spatial self-shielding effect. For new absorber, the concentration of ^{10}B in 90% ^{10}B enrichment B_4C is about 4.5 times of that in natural B_4C while its micro-cross-section is about 50 % of that in natural B_4C .

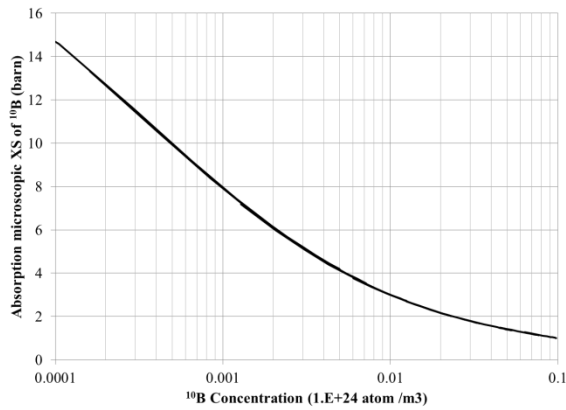


Fig 4. Variation of ^{10}B effective microscopic cross-section with ^{10}B concentration

As shown in Fig 5, the absorption ability of 90% ^{10}B enrichment B_4C increases only about 125 % by comparing with natural B_4C . The absorption ability of ^{10}B decreases under irradiation. For high ^{10}B enrichment B_4C , its initial spatial self-shielding effect is important but it's reduced with depletion of materials that slows down the degradation of control rods' efficiency. The loss of efficiency in lower ^{10}B enrichment B_4C is more important and hence it should be computed in details.

The burnable poisons (BP), independent to control rods system, are designed to compensate core's reactivity loss by its depletion, and hence decrease the insertion depth of control rods. The application of BP would reduce the surplus reactivity from CRs in CRW accidents or bring new degree of freedom in core designs such as increase of cycle length. Furthermore, the efficiency requirement and the movement of control rods during operation would be reduced. BP requires absorbers with enough anti-reactivity at beginning but high depletion kinetic and small residual anti-reactivity at the end. As shown in Fig 4, the lower enriched B_4C has much higher microscopic cross-section. Although their initial macroscopic cross-section is small, their variation is close to natural and high ^{10}B enrichment B_4C . From this point of view, lower enriched B_4C is more suitable for BP purpose.

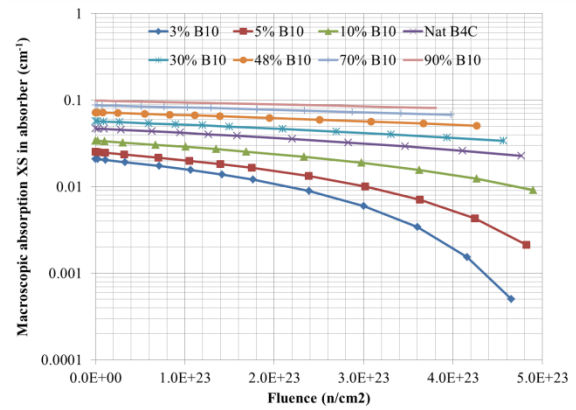


Fig 5. Variation of ^{10}B macroscopic cross-sections with fluency accumulated in absorber

IV.B. Different materials

In this section, B_4C in the original CSD design is replaced by different absorber materials. These different designs are calculated firstly by APOLLO3 TDT solver in cluster with fuel at lattice level and then APOLLO3 MINARET solver in SFR-V2B core.

In this works, complete chains of these isotopes are used. For instance, Lu, Hf, Ta and W are considered in the evolution of Hafnium. Fig 6 and Fig 7 show variation of concentration and macroscopic cross-sections in absorber with fluency accumulated according to sub-assembly calculation. The absorptions for hafnium are principally caused by (n, gamma) which generates higher order hafnium. The Hf181 is also generated in this chain while its half-life is only about 42 days and hence transform to Ta181 by beta- decay. As shown in Fig, the total concentration of these isotopes is constant which proves the conservation of materials. The most important decrease in concentration and in absorption ability is raised from disappearance of Hf177. The absorption cross-sections of Hf180 are much less important while its proportion is about 35 % in the natural hafnium. Although the concentration of Ta and W generated from (n, gamma) and beta- reactions are not significant, their absorption ability becomes non negligible.

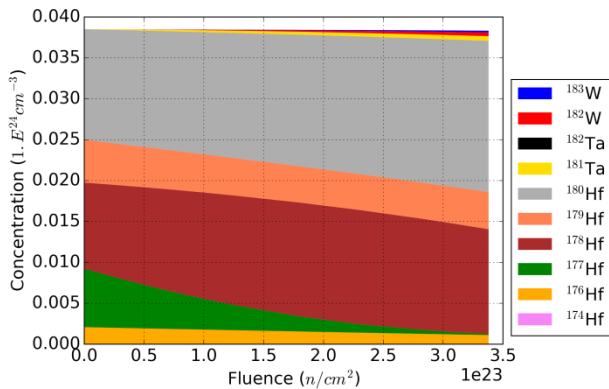


Fig 6. Variation of absorber compositions with fluency

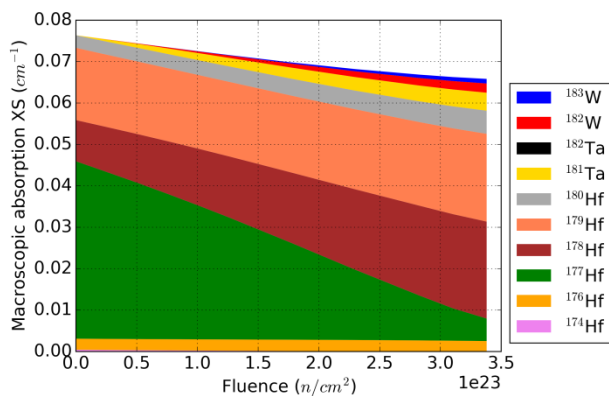


Fig 7. Variation of macroscopic cross-sections with fluency accumulated in absorber

In the core calculation, the natural B₄C in all CSD is replaced by alternative materials. The efficiency of all control rods insertion and solely CSD2 25 cm insertion are presented in Table 2. Among these materials, HfH_{1.62} has highest efficiency and least reactivity loss. The efficiencies of Eu₂O₃ and HfB₂ are close to natural B₄C with a slight slower degradation kinetic.

However, the efficiency of metallic Hf, Gd₂O₃ or Dy₂TiO₅ is not comparable with natural B₄C. Although these rare earth elements have longer depletion chain than B₄C, their improvement on reducing loss of reactivity worth is not significant as hafnium. The evolution of isotopes relieves more importantly spatial self-shielding effect in B₄C and HfH_{1.62} because the outer region depleted firstly and then behaves as ‘moderator’ to slow down the neutrons that might improve the absorption ability in the inner region.

All rods insertion should be able to shutdown reactors at any moment. The results in Table 2, is calculated only at BOEC. According to our calculation, with evolution of core, the power distribution shift from outer core to inner core and hence the efficiency of all control rods insertion at EOEC is more important than that BOEC. The reactivity loss of this efficiency is less significant because it comes from both CSD and DSD. However, some designs still not satisfy the requirement. Hence, we propose axially mixed control rods where the insertion part is replace by material with high residence to depletion and other part by material with high absorption ability. Several control rods S/A designs already adapt control rods with two axial regions with different ¹⁰B enrichment B₄C. However, the axial connection with different materials should be investigated firstly and then detailed evolution of designs.

Table 2. Efficiency of different materials

	Reactivity worth of CSD2 25 cm insertion			Reactivity worth of all control rods insertion		
	BOL	EOL	Loss	BOL	EOL	Loss
Nat. B ₄ C	510	432	-15%	6396	6030	-6%
HfH _{1.62}	672	642	-4%	7955	7691	-3%
Eu ₂ O ₃	457	403	-12%	5880	5565	-5%
Nat. HfB ₂	442	381	-14%	5780	5449	-6%
Hf	252	235	-7%	4141	3984	-4%
Gd ₂ O ₃	248	217	-12%	4136	3924	-5%
Dy ₂ TiO ₅	210	186	-12%	3815	3636	-5%

The ability to compensate reactivity loss of different materials is shown in Fig 8. This figure depend not only the characteristics of these absorbers but also the ‘architecture’ of control rods such as the number of control rods S/A, their position in the core, the insertion depth and so on. However, if the neutron spectrum is similar, the relative relation between different material and different ¹⁰B enrichment would be still valuable. This figure is based on SFR-V2B core calculation but the lattice calculation in also able to get similar results because the reactivity worth of control rods in core is proportional to the macroscopic cross-section calculated with Fig 3.b.

If core has low reactivity loss, natural B_4C even “depleted” B_4C is able to compensate reactivity loss. Other alternative material are suitable but their economic performance should be evaluated because rare earth elements are more expensive than natural B_4C .

High reactivity loss core requires enriched B_4C . Reactivity worth of B_4C does increase slowly with ^{10}B enrichment. Furthermore, margin to melting will limit the residence time of enriched B_4C because its power density is proportional to ^{10}B enrichment. One solution is presented in next section where small pins design to improve heat transfer and moderators to homogenize absorption distribution and to save enriched B_4C investment. Another solution would be to replace B_4C with other material such as HfB_2 . The thermal conductivity of HfB_2 is much more significant than B_4C . The efficiency of natural HfB_2 is slight smaller than natural B_4C but their efficiencies would become closer with increase of ^{10}B enrichment. The third solution may be radially mixed designs where only certain B_4C pins replaced by alternative materials with higher margin to melting. The designs and evaluation of radially mixed control rods is in progress.

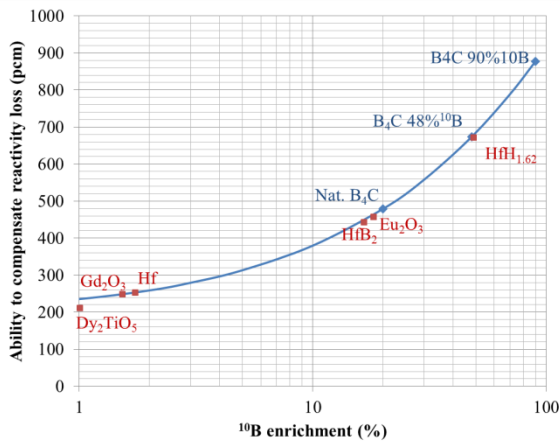


Fig 8. Ability to compensate cycle reactivity loss of different materials

IV.C. Moderator

As shown in Fig 9, the number of absorber pins is increased from original designs 37 pins to 127 pins with same volume of absorber and

structure. Furthermore, moderator pins replace 19 small absorber pins and hence it saves about 15 % investment of absorber.

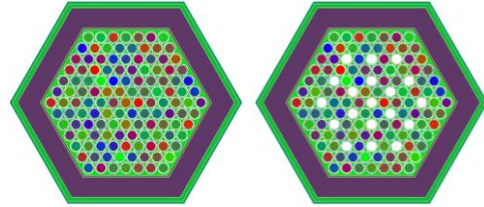


Fig 9. Control rods with small pin size (left) and control rods with moderator pins (right)

This design is charged with different absorber and moderator and is calculated in the same algorithm as previous designs. As shown in Table 3, the switch from big pin size to small pin size increase slightly the efficiency of control rods. ZrH_2 increases all absorber’s absorption ability especially for metallic Hf. However, the use of moderator increases also the reactivity loss of control rods because their higher average absorption rate. $HfH_{1.62}$ has equivalent efficiency as 50 % ^{10}B enriched B_4C and very small reactivity loss but its melting temperature is close to SFR operation temperature. The direct mix of Hf and H is more effective than the introduction of independent moderator pins. However, as a metal, it has more flexibility on the geometries and introduction of moderators. As shown in Fig 10, several innovative geometries of control rods are proposed and would be evaluated in near future.

The BeO increase the average absorption rate in absorber but it is not able to increase the total absorption in control rods S/A because it also replace a part of absorber. However, it is also able to homogenize the distribution of absorption with adequate positioning. In the future, the influence of moderator on the temperature distribution in the control rods under irradiation should be computed especially for high ^{10}B enrichment B_4C .

Table 3. Efficiency of different designs with small pin size and moderator

Absorber	Moderator	BOL	EOL	Loss
Natural B_4C	Non	518	439	-15%
B_4C	BeO	497	408	-18%

	ZrH ₂	549	459	-16%
Hf	BeO	253	233	-8%
	ZrH ₂	344	321	-7%
Nat. HfB ₂	ZrH ₂	493	415	-16%

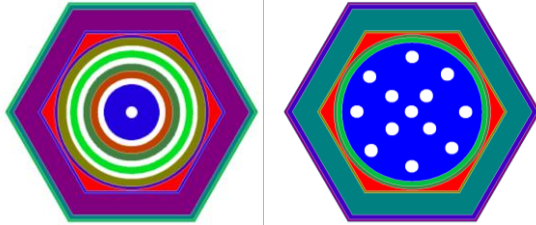


Fig 10. Innovative geometries for control rods with metallic Hf

V. CONCLUSIONS

Current control rods designs use B₄C as absorber but with multi limitations regarding for its safety margin, residence time and economic performance. Several innovative designs are proposed. Base on the validated APOLLO3 calculation schemes and Monte-Carlo codes, these designs are evaluated in our work.

The spatial self-shielding effect limits the absorption ability of high ¹⁰B enrichment B₄C but also slows down its degradation. With high-level capture cross-section, lower enriched B₄C is the most suitable materials for burnable neutrons poisons in SFR. Thanks to moderator, Eu₂O₃ and HfB₂ have improvement safety characteristics and equivalent efficiency to natural B₄C that would replace the B₄C in low reactivity loss cores. HfH_{1.62} has equivalent efficiency as 50 % ¹⁰B enriched B₄C and low reactivity loss. Moderator may save investment of expansive absorber and even improve reactivity worth. It homogenizes reaction distribution and hence reduces the absorption peak.

Several design directions are also proposed in this paper such as burnable neutrons poisons using lower enriched B₄C, radially or axially mixed control rods to improve local characteristics and innovative pins design for Hf. In the future, these designs will be studied in depth combining with more moderator designs and thermodynamic calculation.

ACKNOWLEDGEMENTS

The authors would like to thank the APOLLO3 development team for their efforts in developing the code. APOLLO3 R is a registered trademark of CEA. We gratefully acknowledge AREVA and EDF for their long term partnership and their support

NOMENCLATURE

GIF Generation IV International Forum
 MOC Method of Characteristics

REFERENCES

- [1] I. L. Pioro, “2 - Introduction: Generation IV International Forum,” in *Handbook of Generation IV Nuclear Reactors*, Woodhead Publishing, 2016, pp. 37–54.
- [2] F. V.-P. MARSAULT–Marie-Sophie, C.-B. B. CONTI, P. S.-C. V. FONTAINE, N. D.-L. MARTIN, and A.-C. S. VERRIER, “Pre-conceptual design study of ASTRID core,” presented at the ICAPP12, Chicago, USA, 2012.
- [3] M. Chenaud *et al.*, “Status of the ASTRID core at the end of the pre-conceptual design phase 1,” *Nucl. Eng. Technol.*, vol. 45, no. 6, pp. 721–730, Nov. 2013.
- [4] P. Sciora *et al.*, “Low void effect core design applied on 2400 MWth SFR reactor,” in *Proceedings of ICAPP*, 2011, pp. 2–5.
- [5] B. Fontaine, N. Devictor, P. Le Coz, A. Zaetta, D. Verwaerde, and J.-M. Hamy, “The French R&D on SFR core design and ASTRID Project,” presented at the Proceedings of GLOBAL 2011, Makuhari, JAPAN, 2011.
- [6] B. Fontaine, V. Marc, P. Sciora, and C. Venard, “ASTRID: an innovative control rod system to manage reactivity,” presented at the ICAPP 2016, San Francisco, California, USA, 2016.
- [7] D. Blanchet and B. Fontaine, “Control Rod Depletion in Sodium-Cooled Fast Reactor: Models and Impact on Reactivity Control,” *Nucl. Sci. Eng.*, vol. 177, no. 3, pp. 260–274, Jul. 2014.
- [8] L. Dujčiková and L. Buiron, “Development and analysis of SFR control rod design,” *Int. J. Phys. Math. Sci.*, vol. 2, 2015.
- [9] A. E. Waltar, D. R. Todd, and P. V. Tsvetkov, Eds., *Fast Spectrum Reactors*. Boston, MA: Springer US, 2012.
- [10] R. Sasaki, S. Ueda, S.-J. Kim, X. Gao, and S. Kitamura, “Reaction behavior between B4C, 304 grade of stainless steel and Zircaloy at 1473 K,” *J. Nucl. Mater.*, vol. 477, pp. 205–214, Aug. 2016.
- [11] M. Akiyoshi, T. Yano, Y. Tachi, and H. Nakano, “Saturation in degradation of thermal diffusivity of neutron-irradiated ceramics at $3 \times 10^{26} \text{n/m}^2$,” *J. Nucl. Mater.*, vol. 367–370, pp. 1023–1027, Aug. 2007.
- [12] Gérald Rimpault, Danièle Plisson, Robert Jacqmin, Jean Tommasi, and Robert Jacqmin, “THE ERANOS CODE AND DATA SYSTEM FOR FAST REACTOR NEUTRONIC ANALYSES,” presented at the PHYSOR 2002, Seoul, Korea, 2002.
- [13] J. Y. Moller, J. J. Lautard, and D. Schneider, “Minaret, a deterministic neutron transport solver for nuclear core calculations,” presented at the M&C 2011, Rio de Janeiro, RJ, Brazil, 2011.
- [14] D. Sciannandrone, S. Santandrea, and R. Sanchez, “Optimized tracking strategies for step MOC calculations in extruded 3D axial geometries,” *Ann. Nucl. Energy*, vol. 87, pp. 49–60, Jan. 2016.
- [15] L. Buiron and L. Dujčiková, “Low Void Effect (CFV) Core Concept Flexibility from Self-breeder to Burner Core,” presented at the Proceedings of ICAPP 2015, Nice, FRANCE, 2015.

- [16] E. Brun *et al.*, “TRIPOLI-4®, CEA, EDF and AREVA reference Monte Carlo code,” *Ann. Nucl. Energy*, vol. 82, pp. 151–160, Aug. 2015.
- [17] M. Ma, W. Xiang, B. Tang, L. Liang, L. Wang, and X. Tan, “Non-isothermal and isothermal hydrogen desorption kinetics of zirconium hydride,” *J. Nucl. Mater.*, vol. 467, pp. 349–356, Dec. 2015.
- [18] M. M. Opeka, I. G. Talmy, E. J. Wuchina, J. A. Zaykoski, and S. J. Causey, “Mechanical, Thermal, and Oxidation Properties of Refractory Hafnium and zirconium Compounds,” *J. Eur. Ceram. Soc.*, vol. 19, no. 13, pp. 2405–2414, Oct. 1999.
- [19] H. Guo, G. Martin, and L. Buiron, “Improvement of sodium fast reactor control rods calculations with APOLLO3,” presented at the ICAPP 2018, Charlotte, North Carolina, USA, 2018.
- [20] G. Mignot *et al.*, “Studies on french SFR advanced core designs,” presented at the ICAPP, Anaheim, CA, USA, 2008.